Development of a post-processing method for estimating solidification parameters from finite-element modeling of laser remelting in directed energy deposition of Ni-Mn-Ga magnetic shape-memory alloy single crystals

Tyler Paplham, Jakub Toman, Markus Chmielus
Department of Mechanical Engineering and Materials Science


Tyler Paplham

Tyler is a senior Materials Science and Engineering major from Buffalo, NY. He has worked in the Advanced Manufacturing and Magnetic Materials lab for almost two years. After graduation, he plans to pursue his PhD in Materials Science and Engineering to research materials for sustainable energy generation and transmission.


Markus Chmielus, Ph.D.

Dr. Markus Chmielus has been an Associate Professor in the Mechanical Engineering and Materials Science Department since 2013. He previously worked at Cornell University (postdoc) and the Helmholtz Center for Materials and Energy in Germany (research scientist), and has degrees from the Technical University of Berlin, Boise State University, and the University of Stuttgart in Materials Science and Aerospace Engineering. He now leads the Advanced Manufacturing and Magnetic Materials Laboratory (AM^3), where his group members perform experimental additive manufacturing and post-processing research on functional magnetic and structural metals.

Significance Statement

This work aims to build on previous work in relating the user-controlled laser parameters to the thermal parameters which govern whether a single crystal can be achieved. Establishing a relationship between these two parameter sets will increase the reliability of single crystal production via directed energy deposition.

Category: Computational Research

Keywords: **Finite element analysis, directed energy deposition, additive manufacturing**

Abstract

Directed energy deposition is a subset of laser additive manufacturing which has been suggested as a feasible method for producing single crystals of metal alloys such as Ni-Mn-Ga magnetic shape-memory alloys. However, relating the thermal parameters, specifically the solidification front growth velocity V and thermal gradient G to the operational parameters, specifically the nominal laser power and travel velocity, is challenging. Therefore, this work aimed to use finite-element analysis (FEA) to create thermal models which allow for the determination of G and V for operational parameter combinations. Comparison with experimental data allowed for association of the range of G and V with the samples that best displayed single crystal growth. It was found that a high power and medium-low travel velocity is most likely to result in single crystal growth.

1. Introduction

Directed energy deposition (DED) is a type of laser additive manufacturing in which powdered material is injected via converging jets of an inert shield gas into the laser beam. This simultaneously melts the substrate and incident powder to join the two. DED is particularly attractive for production of macroscopic single crystals, which have numerous material property benefits over their polycrystalline counterparts. Of importance to predicting whether a single crystal is achievable by the user-controlled laser parameters (e.g. laser power, laser travel velocity) are the thermal gradient G and interface growth velocity V. Mathematical models such as that developed by Gäumann et al. have become accepted as an analytical representation of melt pool resolidification. The Gäumann model utilizes the Rosenthal solution, which describes the gradient G for a moving point heat source, to analyze the columnar (corresponding to single-crystal growth) to equiaxed transition (CET) observed in alloy resolidification after melting by such a heat source [1]. For low gradient and high resolidification velocity, the microstructure is expected to be equiaxed, as stray grains will nucleate ahead of the solidification front and inhibit progression of the columnar resolidification front, which is detrimental for single-crystal growth. However, for high thermal gradient and low resolidification front velocity, it is possible to prevent stray grains from nucleating. This allows the columnar front to advance uninhibited and a single crystal to be produced [2,3]. It should be noted that this solution is an approximate one, as it not only assumes a semi-infinite substrate but neglects the significant effects of latent heat of phase change and circulation within the melt pool, which are very difficult to model analytically.

An important parameter used to predict columnar growth in the Gäumann model is G^n/V, where n is a material-specific constant determined from thermodynamic and kinetic analysis. This parameter is useful because it is independent of the vertical depth within the melt pool. A threshold value of G^n/V at which the phase fraction of grains nucleated ahead of the solidification front is exactly half can be used to delineate between columnar and equiaxed growth. The value of n used by Gaümann is 3.4, but the value for the Ni-Mn-Ga system is yet. However, for the present, n = 3.4 will be used, allowing the literature threshold of $G^{3.4}/V$ = 2.7 x 10^{24} [$K^{3.4}m^{-4.4}s$] to serve as an approximate indicator of single crystal growth.

Finite element analysis (FEA) provides several distinct advantages over analytical models. Because an FEA model must have finite boundaries, the effects of finite body size and the heat transfer boundary conditions are accounted for, unlike the semi-infinite case of the analytical model. Conversely, the FEA model has important limitations. Whereas the analytical model can return the growth velocity and gradient as continuous functions of position, the FEA is by definition discrete, and thus functions are very difficult to obtain. Since many of the aforementioned complicating effects (phase change, circulation) are similarly infeasible to represent in FEA, this method cannot be expected to accurately calculate the magnitude of the growth velocity and gradient. Still, so long as only the input travel velocity and nominal power are varied between runs, the model should serve to rank the experimental parameter combinations by their solidification parameters. By comparison with the ranges posited by the analytical solutions, it may then be predicted which combinations are most likely to result in a single crystal. It is hypothesized that the value of $G^{3.4}/V$, and thus likelihood of a single crystal, will be maximized at a parameter combination with middling values of laser power and travel velocity.

2. Methods

The experimental substrate was an austenitic $Ni_{51}Mn_{24.4}Ga_{24.6}$ single crystal. The substrate was a rectangular prism with approximate dimensions of 3.8 mm in the laser travel direction x 2.7 mm deep x 15 mm in the transverse direction. Eight combinations of laser power and travel velocity were used to create eight parallel tracks (see first column of Table 1). Finite-element analysis was carried out using ANSYS Workbench and ANSYS Mechanical with the Moving Heat Source extension (version 4.1). This extension enabled the modeling of a moving Gaussian heat source. The deposition of new powder was excluded so as to determine only behavior caused by the melting and re-solidification of the existing substrate. Temperature-dependent quantities for Ni_2MnGa, specifically density ρ, thermal conductivity k, and specific heat C_p were obtained from Smith et al. (ρ) and Brillo et al. (k, C_p), and were input into ANSYS as tabular functions [4,5]. The model was made to be slightly larger (4 mm x 3 mm x 16 mm) than the experimental substrate to facilitate uniform meshing. The model consisted of a fine-mesh central section (0.02 mm spacing) for high accuracy in/near the melt pool surrounded by a coarse-meshed section (1 mm spacing) to reduce runtime.

A beam radius of 0.285 mm was chosen based on specifications for the Optomec LENS used to carry out the experimental DED, although this is an approximation as a truly Gaussian heat distribution does not have a finite boundary. For each run, the laser power and travel velocity were chosen as in the experimental setup. The nominal powers given in Table 1 were attenuated by an absorptivity factor estimated by averaging the ratios of the experimental cross-sectional areas of each melt pool to those of models with corresponding parameters but perfect absorptivity. This resulted in an estimated absorptivity of $\alpha \approx 0.266$. Several additional boundary conditions were added as heat sinks: convection to various degrees across the top surface and sides of the model, conduction through the bottom surface to represent heat loss to the mount, and a radiation condition. After the solution was completed, a time step corresponding to the laser being approximately halfway down the track was chosen (as this most resembles a steady state) and the relevant temperature and directional heat flux data was exported to MATLAB.

Since the thermal gradient is steep relative to the mesh spacing, it was assumed that the melt pool boundary could be defined to sufficient accuracy as all nodes within a small range (± 2 K) of the solidus temperature (1100 K). A Delaunay triangulation method, which is advantageous because it avoids “splinter triangles”, was used to interpolate a surface from the nodes. For each triangular element, the normal vector was calculated, normalized and dotted with the laser travel velocity to calculate local solidification front velocity (see Fig. 1). The gradient was determined by exporting the directional heat flux along each of the primary axes of the model at every node at the same time step at which the temperature data was collected. Since the exact conductivity used by the simulation at every

given point was unable to be exported, the Brillo data was directly imported to MATLAB, where linear interpolation was used to approximate the instantaneous conductivity for each given point. Since the heat flux q'' and conductivity k are known, the gradient $G = \nabla T$ can be found from Fourier's law of thermal conduction $q'' = -k\nabla T$.

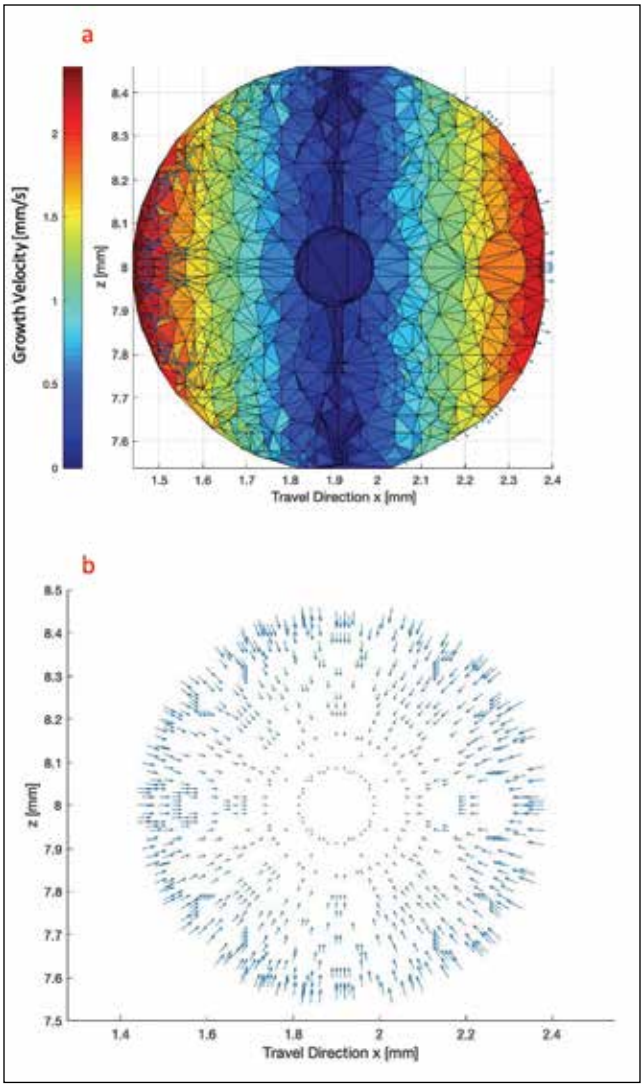

Figure 1: Top view of melt pool for 250 W – 2.5 mm/s track. (a) Growth velocity V with normal vectors. Color corresponds to magnitude of growth velocity. (b) Thermal gradient G vectors at the boundary of the melt pool.

Therefore, the experimentally observed transition between vertical growth and growth parallel to laser travel direction was able to be predicted from the model by the depth in the melt pool that the x-component of the gradient is greater than the z-component. However, this transition is continuous in experiment, and as such the point where "horizontal" begins is only an estimate.

3. Results

Laser Parameters [W – mm/s]	G × 10^3 [K/mm]	V [mm/s]	$G^{3.4}/V \times 10^{24}$ [$K^{3.4}m^{-4.4}s$]
100-0.5	3.4488	0.1223	138.25
100-1	3.8904	0.1372	185.62
100-2.5	4.1990	0.3587	92.025
200-2.5	2.5040	1.1087	5.5883
250-1	2.0650	0.4424	6.6816
250-2.5	2.6000	1.0621	6.0922
250-5	2.9782	2.0374	5.0389
250-10	3.3893	3.7297	4.2727

Table 1: Average thermal gradients and growth velocities calculated for each of the parameter combinations, denoted in power-velocity form, along with the $G^{3.4}/V$ value.

It can be seen from Table 1 that the average growth velocity was only a fraction of the laser travel velocity, and that the gradient generally increased with laser travel velocity. For a given travel velocity, the gradient tended to decrease significantly with increasing laser power. The calculated values of $G^{3.4}/V$ were all found to be above the threshold 2.7 x 10^{24} except for 250 W, 1 mm/s, predicting that all experimental samples should display predominantly columnar growth, which indeed is what was observed. The predicted transition between vertical and horizontal growth is compared to the experimental results in Table 2 via comparison of the depth fraction of vertical growth relative to the melt pool depth. Note that no experimental fraction was determined for any of the 100 W tracks because no melt pool was observed as a result of this laser power.

Laser Power [W]	Travel Velocity [mm/s]	Sim. Fraction	Exp. Fraction	Percent Error
100	0.5	0	-	-
100	1.0	0	-	-
100	2.5	0	-	-
200	2.5	0.5833	0.5834	-0.0002
250*	1.0*	-	-	-
250	2.5	0.4375	0.4209	3.944
250	5.0	0.4643	0.5573	-16.69
250	10.0	0.5000	0.3206	55.95

*This sample had highly irregular melt pool shape likely due to proximity to edge of substrate resulting in less material to act as a heat sink. No clear vertical region was observable.

Table 2: Depth fraction of vertical growth as predicted by simulation vs. the experimentally observed depth fraction. Percent error is defined here as deviation from the experimental depth.

4. Discussion

The results in Table 1 are in strong agreement with the range of V and G values predicted for DED resolidification by Gäumann. This was expected for the growth velocity, as this is merely determined by the orientation of each infinitesimal area of the solidification front relative to the laser travel velocity. However, the fact that the thermal gradients match the predicted magnitude of 10^6 – 10^7 K/mm indicates that this model is a satisfactory representation of the analytical model used in the literature [2]. All eight parameter combinations resulted in a melt pool, despite the fact that the three 100 W tracks did not display any evidence of remelting in experiment. This can be attributed to the fact that the model does not factor in latent energy of fusion, i.e. without any additional energy cost for phase change. It is likely that, had this factor been able to be included in the model, no melt pool would have been observed in simulation. Even if there was some melting experimentally, the simulation results show an extremely shallow melt pool (<60 m) with a uniformly vertical thermal gradient orientation. This indicates that solidification might occur with an entirely planar interface, which would be difficult to observe under optical microscopy. High gradients were generally associated with high laser velocity. This means that there is no clear optimum highest gradient/lowest velocity combination for single crystal growth, with best results likely arising from a medium-high gradient and a medium-low velocity. If "optimal" is simply defined here as the maximum $G^{3.4}/V$ value, then 250 W – 1 mm/s is the optimum, which satisfies the prediction of a medium-high gradient and medium-low velocity. The 100 W tracks had higher $G^{3.4}/V$ values, but again this power is insufficient to induce melting at least at the travel speeds tested. As mentioned, all parameter combinations had a $G^{3.4}/V$ index greater than the threshold value of 2.7 x 10^{24} [$K^{3.4}m^{-4.4}s$]. The lowest reported value occurred in the 250 W – 10 mm/s run, which was also the only parameter combination which in experiment showed a transition from vertical growth not to horizontal cellular growth but to equiaxed dendritic growth. This is evidence that the $G^{3.4}/V$ index for this parameter combination has crossed some threshold value past which the growth mode has changed. A more conclusive explanation is limited by the fact that the correct value of n is not known for this particular alloy. As defined originally by Hunt and later utilized in the Gäumann model, this parameter is dependent on the linearity of the phase boundaries, the shape of the dendrite tips, and the Péclet number. While the chosen value n = 3.4 for the alloy in Gäumann is meant to be more realistic value than n = 2 used by Hunt (which assumes linear phase boundaries and hemispherical dendrite tips), the characteristics of the controlling phenomena would have to be determined for $Ni_{51}Mn_{24.4}Ga_{24.6}$ for a more exact definition of n [2].

As can be seen, the model was relatively accurate in predicting the depth of transition at low velocities, but less so at high velocities. It is predicted that the 250 W – 10 mm/s track was associated with such a high error because the growth mode changed during processing, resulting in this metric no longer being a good predictor of transition. Still, the subjectivity of where the continuously changing growth direction is considered "horizontal" makes it incredibly easy for errors this large to arise. Additionally, while the general temperature distribution did show an elongated "tail" in the wake of the melt pool, the melt pool itself remained relatively circular. Since it is expected that the melt pool should also have a tail whose size depends on the magnitude of the velocity, this suggests that the convection and radiation boundary conditions were too high; this is unsurprising as they were somewhat arbitrarily applied.

5. Conclusion

Using the FEA model developed in ANSYS Workbench, it was found that since high thermal gradients were generally associated with high solidification velocity, there is no highest gradient/lowest velocity combination which maximizes $G^{3.4}/V$ and by extension probability of achieving a single crystal. Instead, maximal $G^{3.4}/V$ was found in the 250 W – 1 mm/s run, satisfying the hypothesis of a medium-high gradient and medium-low velocity. Future work could determine a more accurate value of n for this material system, which would enable a more reliable prediction of the parameters resulting in magnetic shape-memory alloy single crystal production.

6. Acknowledgements

This project was funded by NSF grant #1808082, the Swanson School of Engineering, and the Office of the Provost. This work was performed in part at the Materials Micro-Characterization Laboratory. Additional acknowledgement to the rest of the Advanced Manufacturing and Magnetic Materials lab for support during this project.

7. References

[1] Kurz, W., Bezençon, C., Gäumann, M. (2001) "Columnar to equiaxed transition in solidification processing". *Sci.& Tech. Adv. Mat.,* **2** (pp. 185-191)

[2] Gäumann et al. (2001) "Single-crystal laser deposition of superalloys: processing-microstructure maps". *Acta Materialia,* **49**, *6* (pp. 1051-1062)

[3] Gäumann et al. (1997) "Nucleation ahead of the advancing interface in directional solidification". *Mat. Sci. & Eng.* **A226-228** (pp. 763-769)

[4] Smith et al. (2014) "Rapid actuation and response of Ni-Mn-Ga to magnetic-field induced stress". *Acta Materialia*, **80** (pp. 373-379)

[5] Brillo et al. (2011) "Thermophysical properties and thermal simulation of Bridgman crystal growth process of Ni-Mn-Ga magnetic shape memory alloys". *Int. J. Heat & Mass Trans.* **54** (pp. 4167-4174)